Anti-Brownian electrokinetic trapping of phospholipid vesicles

by

© Corey Kelly

A thesis submitted to the

Department of Physics and Physical Oceanography

in partial fulfilment of the

requirements for the degree of

Bachelor of Science (Honours)

Department of Physics and Physical Oceanography

Memorial University

March 2009

St. John's Newfoundland and Labrador

Abstract

Phospholipids are polar compounds found in biological matter. Their amphiphilic nature causes them to form bilayers, which can fold over onto themselves, forming bubble-like structures called vesicles. The physical mechanism of vesicle formation and the physics of many vesicle properties are not well understood. Much work has been done to optimize vesicle formation, both in increasing average size, and minimizing the distribution of sizes so that the size dependence of vesicle properties can be studied. It has also been found that the formation of vesicles is enhanced by the presence of an AC electric field.

Following closely the work of Estes and Mayer [10], vesicles are electroformed from spin-coated lipid layers. By using lipid-soluble dye, the vesicles are imaged using fluorescence microscopy. We are studying methods of characterizing a single vesicle and its properties by attempting to electrokinetically trap it in one dimension using DC electric fields.

Our preliminary studies of electrokinetic mobility of vesicles produced unexpected types of motion. We arrive at the conclusion that changes need to be made to our cell design to study the electrokinetics of vesicles. We intend to remedy this by miniaturizing our trap, and performing our electroformation and trapping in separate cells, allowing each cell to be more tailored to its own purpose.

Acknowledgements

I'd first and foremost like to thank my family for their support and constant encouragement. I dedicate this thesis to them.

My friends and roomates have been the ones who have put up with me through the stressful times associated with an honours degree. For that, I thank them. When it comes to this thesis specifically, I would like to thank Andrew Chapman for his numerous bits of advice, recommended sources, and general help putting the *bio* in biophysics. I thank the honours room crowd for their assistance in the furthering of my mastery of procrastination. I also thank my girlfriend Caleigh Macdonald for continual encouragement, which was immensely effective, even from such a great distance.

I would like to thank our entire research group for a good time, and plenty of useful advice. Andrew Bartlett for fun times with tubes in the synthesis lab during the summer. Amit Agarwal for the most thorough tutorial on cell assembly I could ever hope to receive. Hughie Newman for helping me feel like part of the physics department, re-introducing me to the art of yo-yo, and some much appreciated last minute IDL assistance. Also, thanks to Marek and Max for assistance with figure 3.5, the photographing of which was apparently a three person job.

Finally, this project would not have been possible without the supervision, advice, and encouragement of Dr. Anand Yethiraj. For introducing me to a field of physics I might have never known, and helping me develop a working knowledge of some small aspect of that field. Your passion for your own work has sparked something in me that I didn't expect when I started this project. Thank You.

Contents

List of Figures

List of Tables

Chapter 1

Introduction and Background

1.1 Particle Trapping

1.1.1 Motivation: Brownian Motion

It was Albert Einstein who proposed the theory (as we know it) for the "jittery", random motion of objects in a fluid [9]. Essentially, the thermal excitation of the water molecules makes them continually collide with any objects in their vicinity, causing random motion with an associated energy on the order of $k_b T$ (Boltzmann's constant and the absolute temperature) and a average displacement proportional to $\sqrt{time}$ [9]. This motion is known as Brownian motion and becomes quite apparent as we observe increasingly microscopic systems. Because the motion is a consequence of thermal fluctuations, it is unavoidable at all non-zero temperatures. Particle diffusion can be limited by decreasing the system temperature (which might not make a significant difference before the phase transition temperature of the solvent) or increasing the viscosity of the solution, but can never be

completely eliminated.

We can usually try to design our system such that more significant sources of particle motion (such as fluid flow or gravitational sedimentation) can be minimized, but to infer the *natural* physical state of a system, Brownian motion must be considered in all analyses. In certain cases this unstoppable motion of the object of interest can cause practical difficulties. For example, a common issue in microscopy is particles diffusing from the field of view or out of the plane of focus. When trying to get high resolution images of a particle, we wish to maximize it relative to our field of view, but in doing so we minimize the amount of time it can be imaged before disappearing from our imaging region. A balance must be struck between quality of data acquired and time over which data can be gathered, and even so there is an upper limit on time scales.

From this physically inevitable struggle arises the somewhat broad term "particle trapping", which encompasses any means by which we can minimize (or eliminate) particle motion.

1.1.2 A Common Trapping Method

Perhaps the most successful and widely known method of particle trapping is the use of a laser beam to create large, localized electric field gradients which attract particles to the beam centre and hold them there. This was first observed experimentally in 1986 and is commonly referred to as an optical trap, or *optical tweezers* [3]. Since this trapping method involves optical manipulation, it is easily integrated into different sorts of microscopy systems, and by time-sharing the laser

focus, multiple particles can be trapped simultaneously.

While this is a tried and tested experimental technique, one can easily imagine situations in which a large field gradient might not be desirable. For any object which doesn't have a rigid structure, the gradient can cause deformation of the particle, compromising the integrity of any result which is shape-dependent.

1.2 Phospholipids

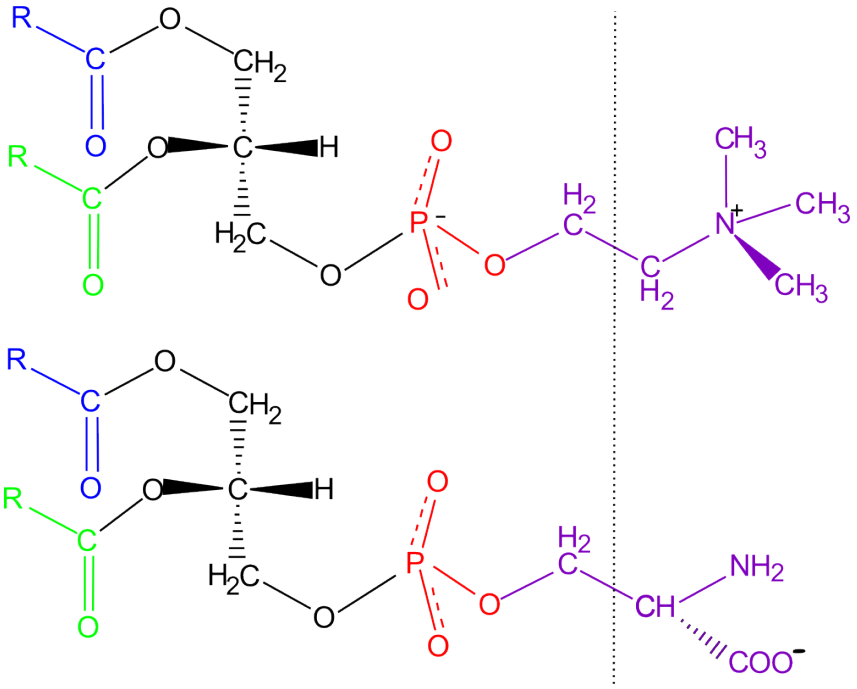

Figure 1.1: The structure of two common phospholipids, phosphatidylcholine and phosphatidylserine(from [18]). Dotted line indicates differing functional group.

Phospholipids are organic compounds consisting of fatty acid chains connected to a polar head containing a phosphate group. Figure 1.1 shows the chemical struc-

ture of two such molecules: Since the headgroups are hydrophilic and the fatty chains are hydrophobic, the molecules as a whole are amphipathic. This asymmetric nature of the molecules gives rise to interesting structural formations when phospholipids are put into solution [11]. This type of self assembly is of great importance to life as we know it, since phospholipid bilayers constitute the majority of cellular membranes in living organisms.

1.2.1 Bilayers and Vesicles

Figure 1.2 illustrates how the phospholipid molecules orient themselves in a bilayer. It is apparent why these structures are energetically favourable, since both the hydrophobic and hydrophilic portions of the molecules are satisfied. Depending on conditions in the solution, and more importantly, the effective volume occupied by the fatty acid chains of the phospholipid relative to the volume of the headgroup, different membrane curvatures are preferred [11]. We will be focusing on a type of structure known as a vesicle (also commonly referred to as liposomes, depending on specific functionality). Vesicles can be thought of as bilayers which have folded over onto themselves, enveloping some volume of water. This structure turns out to be an invaluable asset to studies of biological membranes. Since vesicles are used in the body for intracellular protein transport [13], they have become a common method of delivering drugs to the body that would not normally be inert in a physiological setting [16].

The bilayer membranes constituting vesicles are soft and flexible, so while vesicles prefer to be roughly spherical, the structures can be deformed quite easily.

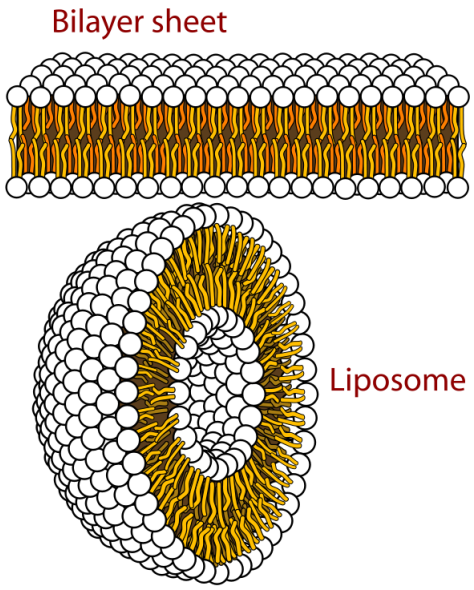

Figure 1.2: Two common structures formed by phospholipids in aqueous solution (from [17]).

They can also be punctured, fused, or completely destroyed if forces are applied to them in particular ways. This is a perfect example of a system as mentioned in section 1.1.2 where the large optical field gradients that are inherent to optical traps might be undesirable. Among many other things, the very fluctuations of the membrane are of great interest, and would be compromised if a large force were to be applied to a localized point on the membrane surface [4]. In addition, optical traps depend on a large refractive index mismatch between the particle of interest and the surrounding solution, so with semi-opaque objects like vesicles, it is common to attach a molecule of gold to the object and trap the gold. A more "gentle" way of holding a vesicle in place for long timescale analyses would be immensely useful.

1.3 Electrokinesis and Electrokinetic Trapping

1.3.1 Electrokinetics

Some of the most interesting behaviour of liposomal membranes occurs when they are exposed to electric fields. Many of the interesting behaviours mentioned in 1.2.1 can be induced by either AC electric fields of varying frequencies or DC field pulses. Processes such as electro-deformation, electro-fusion and electro-poration (the increase in permeability of the lipid bilayer [14]) have all been studied and show that vesicle response to electric fields are quite robust [8].

We hope to take advantage of the strong response of vesicles to electric fields in a attempt to devise a method to study long timescale properties of vesicles, and lipid bilayers in general.

1.3.2 Our Goal: ABEL Trapping

We intend to study the electrokinetic mobility of vesicles, with the ultimate goal of being able to minimize their diffusion by calculating their displacement in real time and offsetting it with electrokinesis. This process has recently been applied to nanoscale objects such as individual molecules in aqueous solution [6], where it is referred to as an "Anti-Brownian Electrokinetic Trap", or ABEL trap. For this process to operate in real time, we must be constantly gathering information and adjusting the DC field to suit the motion of the particle. A schematic of this "feed-back loop" is shown in figure 1.3.

This type of trapping can in principle end our search for a gentle means of trap-

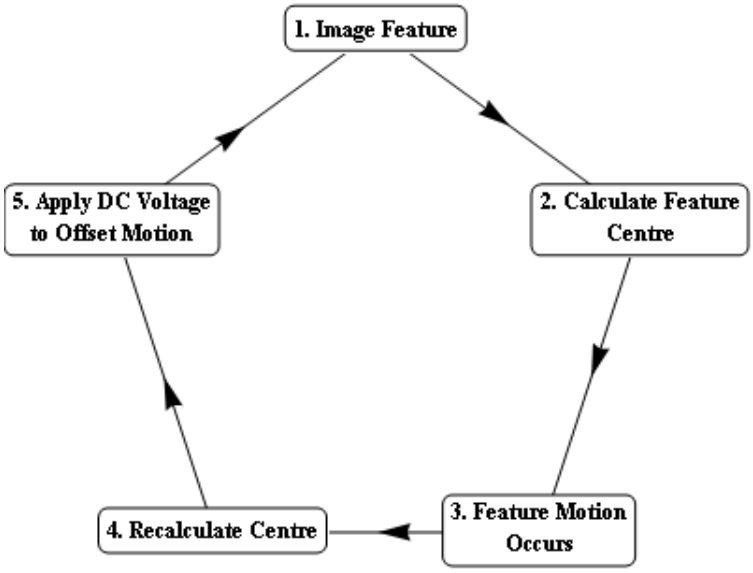

Figure 1.3: ABEL Trap Feedback Loop

ping our vesicles. The main sources of mobility in the ABEL trap are (according to [6]) electrophoresis, the motion of charged particles in an applied electric field; and electroosmosis, and induced flow of fluid near a charged surface [11]. Since these both involve non-localized forces acting on the vesicle, we can avoid membrane deformations associated with large force gradients.

It should be noted that ABEL trapping has been successfully applied to lipid vesicles [6], where the vesicles used were on the order of $100\,nm$ in diameter. The behavior of vesicles of this size closely models colloids in that membrane fluctuations can generally be ignored. We will attempt to apply the same trapping technique to vesicles upwards of three orders of magnitude larger, where membrane fluctuations are all but negligible.

In chapter 2 we will discuss our method for formation of phospholipid vesicles.

Chapter 3 details the experimental apparatus we will be using for the ABEL trap, along with the computer software used. In chapter 4, we explore electrokinetic mobility of both colloidal polystyrene, and phospholipid vesicles. A summary of our results, along with conclusions and possible future directions are in chapter 5.

Chapter 2

Vesicle Formation

Given the complex structure and behavior of vesicles, studying them involves first devising a reliable method for their production. Great care must be taken to consistently produce vesicles, and we combine two methods for optimizing this production both in terms of peak size and number of vesicles produced: spin coating (section 2.2) and electroformation (section 2.3).

Our method of vesicle production follows very closely the work of Estes and Mayer [10], who studied the optimization of vesicle formation from spin coated lipid layers using a method known as electroformation. Our lipids are purchased in a dry, powdered form from Avanti Polar Lipids. We will deal with two types of lipid, the first of which is L-α-phosphatidylcholine, a phospholipid derived from chicken eggs which Avanti calls EggPC. EggPC is a variant of phosphatidylcholine, which is shown in figure 1.1 This lipid is known to readily form vesicles in aqueous solution [2] and is particularly responsive to electroformation [10]. The second lipid we will be using is phosphatidylserine (PS), which differs principally from

EggPC in that it is an ionic salt. When PS is hydrated, the salt dissociates leaving the lipid portion with a net charge. This charged lipid is shown alongside phosphatidylcholine in figure 1.1. We will be adding PS to our EggPC in low concentrations in the event that the electrically neutral EggPC vesicles do not respond to DC electric fields.

2.1 Solution Preparation

As mentioned, our lipids arrive in a dry, powdered form. For our purposes (i.e. measuring specific masses of lipid to have precise control over solution concentrations), the lipids are much more convenient to deal with in solution. Dissolving the lipid in organic solvents lends itself well to spin coating. This makes mixing of different lipid types at specific ratios simple, and also makes it much easier to mix dyes with the lipid for fluorescence imaging.

The first step in preparing our lipid is to dissolve the solid into our spin coating solution. We use a mixture of chloroform and acetonitrile at a volume ratio of $95:5$, with lipid dissolved at a concentration of $3.75\,mg\,mL^{-1}$. This solution and concentration has been found to produce thin, uniform layers of lipid when spun onto a glass slide [10]. For the solution with pure EggPC, we simply dissolve the lipid in solution at the given concentration, but the EggPC/PS mixture is slightly more complicated to prepare. We wanted to retain the vesicle formation properties of the EggPC while still imparting some net charge on the vesicles, so we decided to add 15% PS to our EggPC, while keeping the concentration of *total* lipid at $3.75\,mg\,mL^{-1}$ in the same solution. This is accomplished by making one solu-

tion of EggPC in chloroform and acetonitrile at a solution concentration *lower* than $3.75\,mg\,mL^{-1}$, then calculating the concentration of PS in chloroform and acetonitrile that would be required such that some ratio of volumes of the two solutions could be mixed to produce a solution containing $3.75\,mg\,mL^{-1}$ total lipid, and a $15:85$ mass ratio of PS to EggPC. This calculation starts with an expression for the total lipid concentration in the final solution, C_f:

$$C_f = \frac{m_{PC} + m_{PS}}{V_{PC} + V_{PS}} \tag{2.1}$$

Where m_{PC} is the mass of EggPC, m_{PS} is the mass of phosphatidylserine, V_{PC} is the volume of the EggPC solution and V_{PS} is the volume of phosphatidylserine solution. Next, we rewrite V_{PC} in terms of concentration and mass (introducing C_{PC}, the concentration of the EggPC solution), and replace all instances of m_{PC} with $\frac{85}{15} * m_{PS}$, from the mass ratio of the two lipids

$$C_f = \frac{m_{PC} + m_{PS}}{V_{PC} + V_{PS}} = \frac{m_{PC} + m_{PS}}{\frac{m_{PC}}{C_{PC}} + V_{PS}} = \frac{m_{PS}\frac{85}{15} + m_{PS}}{\frac{m_{PS}\frac{85}{15}}{C_{PC}} + V_{PS}} \tag{2.2}$$

Solving for V_{PS} and factoring out m_{PS} we arrive at

$$V_{PS} = m_{PS}(\frac{1}{C_f}(\frac{85}{15} + 1) - \frac{1}{C_{PC}}\frac{85}{15}) \tag{2.3}$$

or

$$V_{PS} = \frac{m_{PS}}{3}(\frac{20}{C_f} - \frac{17}{C_{PC}}) \tag{2.4}$$

For example, if it were convenient to mix the EggPC at a solution concentration of $3.5\,mg\,mL^{-1}$ and we had $25\,mg$ of PS to dissolve, we find that V_{PS} is

$$\frac{25\,mg}{3}\left(\frac{20}{3.75\,mg\,mL^{-1}}-\frac{1}{3.5\,mg\,mL^{-1}}\right)=3.97\,mL \tag{2.5}$$

giving a PS solution concentration of $C_{PS}=6.30\,mg\,mL^{-1}$. The volume ratio for the mixing is found using the lipid mass ratio

$$\frac{V_{PS}}{V_{PC}}=\frac{m_{PS}}{m_{PC}}\frac{C_{PC}}{C_{PS}}=\frac{15}{85}\frac{6.30\,mg\,mL^{-1}}{3.5\,mg\,mL^{-1}}=0.318 \tag{2.6}$$

To allow fluorescence imaging of the lipid, we use a dye called coumarin 6, which is soluble in lipid but not in water. This allows a high contrast between our vesicles and the solution around (and within) them. The dye is a solid and must be added to the spin coating solution such that the mass ratio of dye to lipid is approximately 10^{-3}. We want to add dye at this mass ratio while changing the solution concentration as little as possible. First, the saturation point of coumarin 6 in our chloroform/acetonitrile solution is determined by supersaturating a solution, pipetting a known volume off, evaporating the solution, and weighing the solid. The saturation point was found to be $16.5\,mg\,mL^{-1}$. Simple calculations can be used to show how little the dye addition will change our solution concentration. For example, if we had $10\,mL$ of lipid solution, the amount of lipid present would be $37.5\,mg$, and we would thus require $37.5\times10^{-3}\,mg$ of dye. This corresponds to a dye solution volume of

$$V_{DYE}=\frac{37.5\times10^{-3}\,mg}{16.5\,mg\,mL^{-1}}=2.27\,\mu L \tag{2.7}$$

To see how this affects the lipid concentration, we use

$$\frac{\delta C}{C} = \frac{\delta m}{m} + \frac{\delta V}{V} = \frac{\delta V}{V} \tag{2.8}$$

since lipid mass in the solution is constant with the dye addition ($\delta m = 0$). The relative change in lipid concentration is

$$\frac{\delta C}{C} = \frac{2.27 \times 10^{-6} L}{10 \times 10^{-3} L} = 2.27 \times 10^{-4} = .0227\% \tag{2.9}$$

which is a negligible change in terms of our concentration being optimized for spin coating.

All lipid-containing solutions are stored in containers topped up with dry nitrogen to avoid hydration of the lipid, and kept under refrigeration. We also try to keep the dyed solutions out of light to avoid bleaching of the dye.

2.2 Spin Coating

Prior to spin coating, our glass slides must be cleaned following a rigourous process to ensure optimal lipid coverage and minimal contaminant matter. The slides are first rinsed under ethanol twice, each time being dried under a stream of dry nitrogen. We then ultrasonicate the slides in a $50/50$ mixture of chloroform and methanol for approximately 10 minutes. Following sonication, the slides are rinsed twice under methanol, once again being dried under dry nitrogen. Once the slides are clean, they must be spin coated as soon as possible to avoid airborne contaminants settling on them and ultimately being embedded in the lipid layer.

A slide is placed on the spin coating and $100\,\mu L$ of our lipid solution is deposited near its centre. The slide is spun at $600\,rpm$ for $15\,s$, then stored under

vacuum for approximately 1 hour to ensure complete evaporation of the solvent. During this hour, the slide is kept out of light to avoid and bleaching of the fluorescent dye.

Atomic force microscopy (AFM) allowed us to estimate the thickness of our resultant lipid layers. These AFM images are shown in figure 2.1. To obtain these images, we took a dried lipid layer and scribed a line down the centre of it with a razor blade. We then scanned across this line, allowing us to calculate the change in height when the scanning tip moves from the layer to the glass slide.

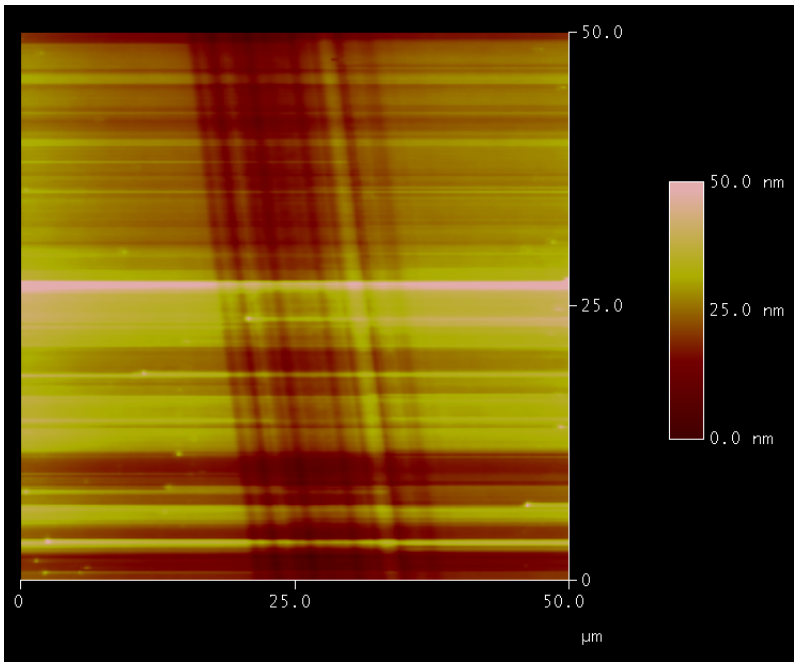

Figure 2.1: Atomic force microscopy image of a spin coated lipid layer.

By calibrating *ImageJ* to associate the image colours with heights using the scale bar on the right, we can select the entire area of the image, and obtain a plot which shows us an average height profile across the scribed line, which is shown in fig-

ure 2.2. By subtracting the low point in this profile from the average of the two sides, we obtain an estimate of the thickness of the lipid layer. This method shows our layers to be approximately $10\,nm$ thick, which is lower than the optimal thickness range of $25nm$-$50nm$ found in [10]. We note that the AFM was not operated in tapping mode as it usually is for soft matter samples, and the data extracted may therefore be of questionable quality.

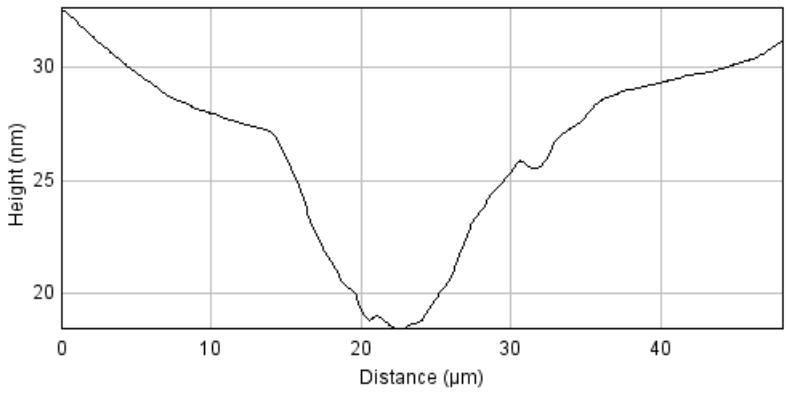

Figure 2.2: Profile across a line scribed in our lipid layer. Extracted from the AFM data in figure 2.1

2.3 Electroformation

The glass slides we use are coated on one side in a compound called Indium Tin Oxide (ITO), which is an optically transparent conducting material. This allows the integration of electrodes into the cell itself, while not affecting our imaging capabilities. The geometry of the cell and the electrodes is further discussed in section 3.4, but for the current discussion it is enough to know that the cell is con-

structed such that an electric field can be created perpendicular to the plane of the lipid layer. Our cells are constructed this way to allow us to employ a technique known as electroformation to further optimize vesicle formation.

Electroformation involves forming vesicles in a low frequency, low amplitude AC field. This technique has long been known to increase the peak size of vesicles [1, 7, 2, 10] however the exact mechanism by which it accomplishes this is not necessarily well understood.

Once the spin coated slides are completely dried, a cell is constructed, filled with water, and a $10\,Hz$ AC current is applied across the cell at a voltage such that the induced field is approximately $1.0\,V\,mm^{-1}$. Vesicles are well formed within 10 minutes, but their size can be further increased by leaving them in the AC field for at least 1.5 hours [10].

Once the vesicles have reached a satisfactory size, the AC field can be removed and the vesicles will be stable enough to image for days, so long as the cell is sealed well enough that the solution doesn't evaporate (see section 3.4.) The coumarin 6 dye allows the vesicles to be excited with a blue laser, and will emit in the green. The vesicles are also visible under white light, or can be imaged using a mercury lamp via fluorescent microscopy.

Electroformation of lipid vesicles worked very well for pure EggPC, and reasonably well for the EggPC/PS mixture. More detailed results are discussed in section 4.1.

Chapter 3

Feedback Loop Construction

3.1 Hardware

The hub of our setup is a Windows XP PC. This machine is equipped with a firewire card to allow communication with our camera (section 3.1.1) and a data acquisition unit (section 3.1.2) which allows us to feedback on our system.

3.1.1 Confocal/Camera

Our cells are imaged on a Nikon Eclipse C1 Plus confocal microscope. We use a technique known as fluorescent confocal microscopy, which has many advantages over conventional bright field microscopy. In the latter, the entire area of interest is illuminated, and the light gathered corresponds not only to the focal plane of interest, but all planes above and below it. Fluorescent confocal microscopy requires that the object of interest be "tagged" with a fluorescent dye, such that it will fluoresce when illuminated with a laser. A clever optical setup within the mi-

croscope is then used to discard any light from focal planes above or below the plane of interest, creating a sharp resolution along the focal axis. By adjusting the objective lens, we can scan along a range of focal planes, and reconstruct the three dimensionality of the sample in a completely non-invasive way [15].

We use a range of objectives, from 4x to 40x, depending on the field of view we require. For example, a 4x or 10x objective is used during electroformation to ensure that vesicle formation is uniform over the majority of the cell. Once the vesicles are formed, we generally switch to a 20x or 40x objective such that a few vesicles (or ideally a single vesicle) can encompass the majority of the field of view. This higher zoom also allows us to resolve interesting behaviour such as vesicle fluctuations which are essential to a complete study of vesicle electrokinetics.

The camera we use to image our cell is a QICAM 12-bit color camera from QImaging (model QIC-F-CLR-12-C.) This camera is mounted on the microscope and claims image capture frequencies of up to $165\,Hz$ with certain binning and resolution settings. This frequency is, in principle, the upper limit on the trapping frequency with our current hardware setup. As mentioned in section 2.3, our vesicles are visible under UV light and can therefore be imaged under a mercury lamp, however the intensity of the light causes the dye to bleach quite quickly. Alternatively, the vesicles are visible under white light, however the highest contrast (and therefore easiest to process) images are obtained with confocal microscopy. Unfortunately, our LabVIEW code cannot yet interface with the confocal software, so for the time being the trap must use images from the camera. That being said, for electrokinetic studies (see Chapter 4) we don't require the voltage output to be tied into the imaging, so we can use the LabVIEW code to control the output voltage,

but image the cell using the confocal.

3.1.2 NI Voltage Input/Output Card

The task of generating time-varying, software-controlled voltages was greatly simplified by the purchase of a National Instruments PCI-4461 data acquisition module. This is a device which we have installed in our microscopy computer, allowing high frequency ($\sim 200kHz$) voltage input and output. The card is controlled by an application called LabVIEW (subsection 3.2.1), and can output arbitrary software controlled waveforms such as sine and square waves, or DC voltages to high precision. The card has two outputs, so the challenge of trapping in two dimensions is simply one of more clever electrode design, and slight modifications to our software code.

3.2 Software and Image Processing

3.2.1 National Instruments LabVIEW

LabVIEW is a software package from National Instruments designed around the concept of a a "visual" programming environment. Its strengths lie in its ability to easily interface different types of hardware, and quickly obtain and analyse data from them. LabVIEW combines all of the elements of a standard programming language (data types, function construction, boolean logic, etc.) in a drag-and-drop environment.

Our main reason for choosing LabVIEW is that for the purposes of our feedback

loop, we require an single interface which allows us to capture images from our camera, process them, carry out calculations, and output a voltage. With drivers for our camera we are able to access our camera from within LabVIEW and capture images at software-controlled intervals. These drivers also give us control of standard camera settings such as exposure and image binning. As add-ons to LabVIEW, National Instruments offers image processing packages (namely, IMAQ Vision) but there are also methods to communicate from within LabVIEW with third party pieces of software (such as the public domain image processing program ImageJ.) This possible linkage greatly expands the image processing abilities at our disposal, and also removes the necessity to code our own particle tracking method, since many image processing applications have built in functions which we can make use of. Finally, since our voltage output card is a National Instruments product, LabVIEW is the easiest interface from which to control it.

3.2.2 Vesicle Tracking Method

Our LabVIEW code in its current state interfaces with ImageJ to perform feature tracking. The LabVIEW code grabs an image from the camera and saves it to the hard disk, then runs ImageJ with a command line argument, feeding it the image file. ImageJ then runs its built in "Particle Analyzer" on the image with and returns the coordinates of the feature to the LabVIEW code via the command line standard output. The parameters of the particle analyzer are adjusted to look for a single, high contrast feature in the image. This obviously works for an idealized feature, but will have to be altered if we wish to eventually allow user control of what

feature is being trapped.

This method works quite well, but the writing of a file to the hard drive and subsequent reading of it make this process somewhat slower than if we had a method of tracking particle centres within the LabVIEW code. Currently, one iteration of the feedback loop takes approximately one second, which would not be fast enough to trap quickly diffusing objects. Fortunately, our vesicles move (relatively) slowly so $1\,Hz$ should be sufficient to trap them.

3.3 ABEL Trapping: Proof of Concept

As a test of whether our hardware and software are all working seamlessly together, we devised a macroscopic "Proof of Concept" setup. Since most objects imaged via microscopy undergo Brownian motion to some extent, the point of the macroscopic model is that we can control the feature motion ourselves and ensure that the feedback loop is functioning exactly as expected.

3.3.1 Setup

Our setup consists of our camera, pointed towards a piece of paper with a small ($\sim 1\,cm$ diameter) black ring drawn on it, and a multimeter connected to our voltage output card. The paper is mounted on a rail to that it can be translated both left and right (x axis) and up and down (y axis) relative to the line of sight of the camera. The LabVIEW code includes a "zero" button to choose a "trapping point" which is essentially the origin of the coordinate system. When the feature is at this point, its offset is 0 along both axes, and no voltage is applied. For the purposes of this

setup, the applied voltage varies linearly with particle offset. This can be modeled by the equation

$$V_x = m(x - x_0) \tag{3.1}$$

where, for our setup, $m = \frac{1}{100}\, V\, px^{-1}$. This slope is chosen such that the whole range of feature motion in the field of view will produce voltages which are within the output range of the DAQ module. If for example the particle is $200\, px$ from the zero point, x_0, the multimeter should read $2.00\, V$. Note that we only "trap" along the x axis for the time being.

The LabVIEW code used for this setup is included in Appendix A.

3.3.2 Results

Put simply, the feedback loop works. When the feature is manually translated along the x axis, a voltage is output proportional to its offset. Figure 3.1 shows a few snapshots of this setup, with the trapping point indicated by a red dot, and the offset indicated by an arrow. As discussed in section 3.2.2, the frequency of the voltage output lags behind the feature motion by approximately one second.

It is also of note that the tracking method ImageJ uses fails when the feature starts to move off the edge of the field of view. This of course would not be an issue in an functional trapping scenario, since the whole purpose of the trap is to isolate the feature to the field of view.

While this test shows that the trap works for an idealized particle, it is likely that the particle tracking method will have to be adjusted for the particle of interest.

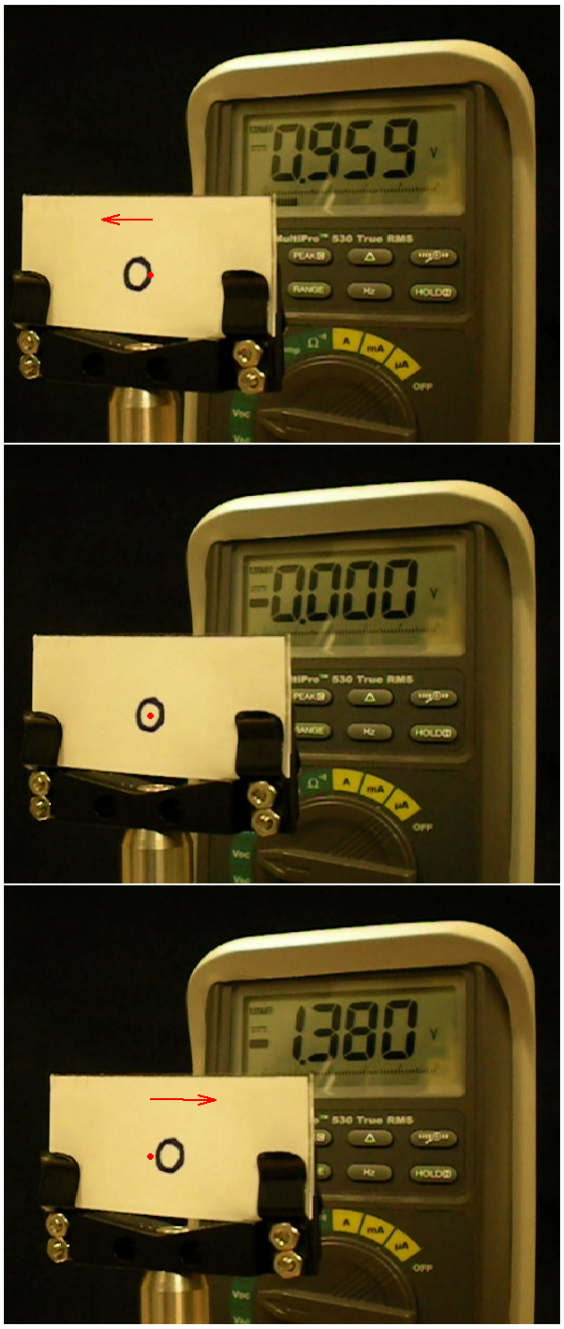

Figure 3.1: Proof of concept setup. Note the change in sign of the applied voltage as the feature is translated to the left and right of the trapping point.

3.4 Cell Construction

3.4.1 ITO Etching

Central to our cell construction are glass slides coated with a thin layer of indium tin oxide (ITO.) This layer is optically transparent and electrically conductive, allowing us to build electrodes into our cells, but still image through them as with regular glass. Since the layer is quite thin, it is easily removed by submerging the slide in hydrochloric acid. By etching certain areas of the ITO while leaving others intact, we can create many different electrode geometries directly on the surface of our glass slide. The actual patterning can be performed using standard photolithography techniques such as the use of photoresist and UV light, which can attain micrometer accuracy in the electrode shape, however we chose a simpler method since we do not require nearly this accuracy. We simply cover the areas of the ITO we do not want removed with tape before putting the slide in HCl. By testing the resistivity of the uncovered areas at various times during the etching process, we can monitor the point when the ITO has been completely removed, and avoid soaking the slide for too long, which could allow acid to leak into areas under the tape and create undesirable features in the ITO.

Using tape on our slides requires the addition of a step to our standard slide cleaning process (see section 2.2). To remove any residue left by the tape, we rinse the slide in acetone and wipe it clean. Once the slide is clean, we use a multimeter to ensure that the electrode geometry is as we intended it to be, making sure that etched regions are indeed void of ITO, and that regions coated in ITO are continu-

ous and still conductive.

3.4.2 Electrode Geometry

Since it is easiest to track particle motion in directions parallel to the plane of the cell, we want to be able to apply voltages parallel to that plane. Also, electroformation is most conveniently carried out in an electric field perpendicular to the plane of the cell, so our electrode geometry was initially designed to allow both of these fields to be applied to the same cell. We accomplish this by creating multiple electrodes and shorting them in different combinations to create different equipotential surfaces, resulting in different field directions. Figure 3.2 shows the pattern in which we etch our ITO slides. The ITO coated regions are shown in green, and the strip in the middle where the ITO has been removed is approximately $1\,mm$ wide. Figure 3.3 is a photograph of an ITO slide etched in the manner shown in

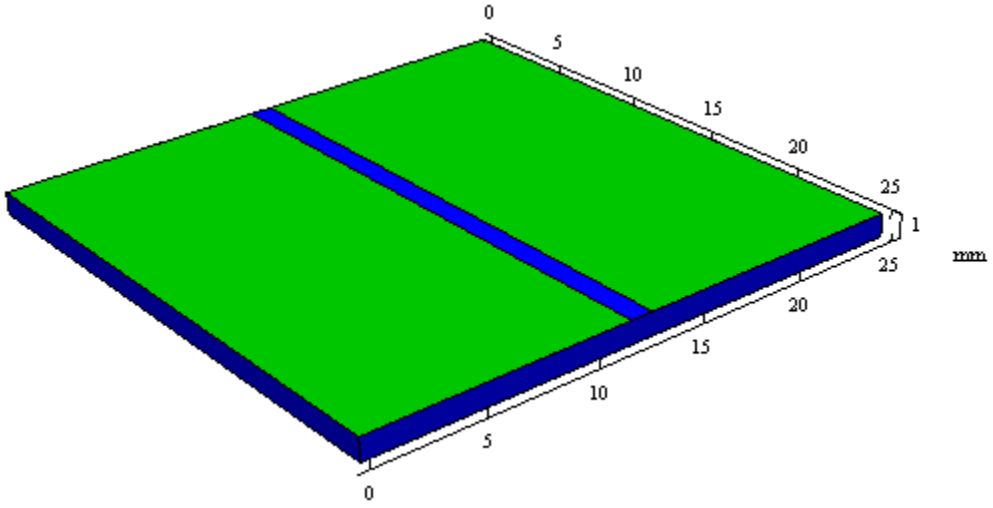

Figure 3.2: ITO etching pattern

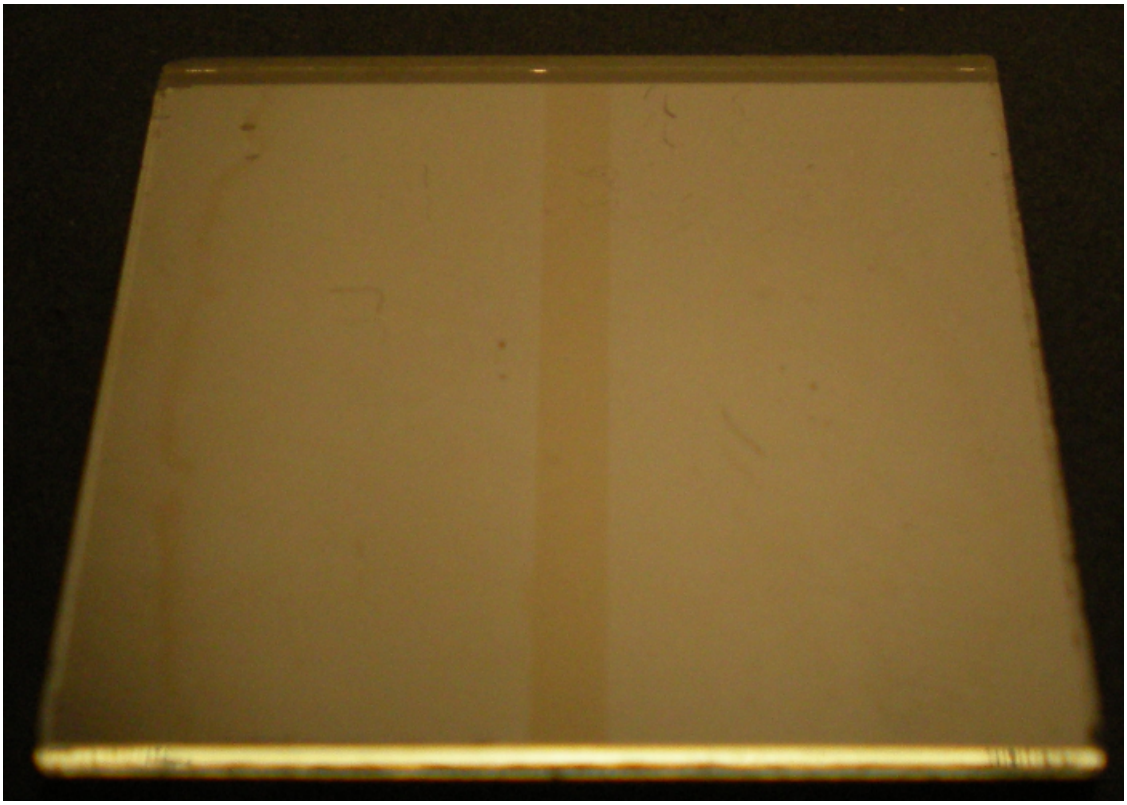

Figure 3.3: A photograph of an ITO slide etched as shown in figure 3.2, with the exception that the etched region in this case is approximately $2\,mm$ wide.

figure 3.2. This picture was taken by illuminating the slide using a uniform white light source, as the difference in reflectance of the etched section is only visible from certain angles.

Both the top and bottom slide are etched in this way, effectively creating four electrodes which are sufficient to create both of the field geometries we require, as explained in section 3.4.3.

3.4.3 Cell Assembly and Field Geometry

Figure 3.4 shows two views of the constructed cell, in which the ITO electrodes are coloured green, spacers are red and electrical leads are connected at points marked with yellow numbers. Our spacers are $1\,mm$ thick, which creates a relatively spacious cell. This allows plenty of vesicle formation to occur, while still having sufficient room to observe diffusion of the vesicles, and maintains the possibility of isolating a single vesicle for trapping. The first step in the assembly of the cell is to attach the bottom plate to a microscope slide using Norland Optical Adhesive 61 (NOA 61). This is an optically transparent glue with a viscosity of $300\,cps$ which cures under UV light. Since our spacers are made from cut pieces of microscope slides, they are positioned so that the factory-machined edge faces into the cell, since perfectly parallel and smooth spacers are less likely to allow bubbles to form in the cell. The spacers are also attached with NOA 61.

The top plate is the one on which we have spin coated the lipid layer. Because of this, the remaining steps in the cell construction must be performed carefully, but as quickly as possible since the lipid will hydrate in open air. When the top plate is

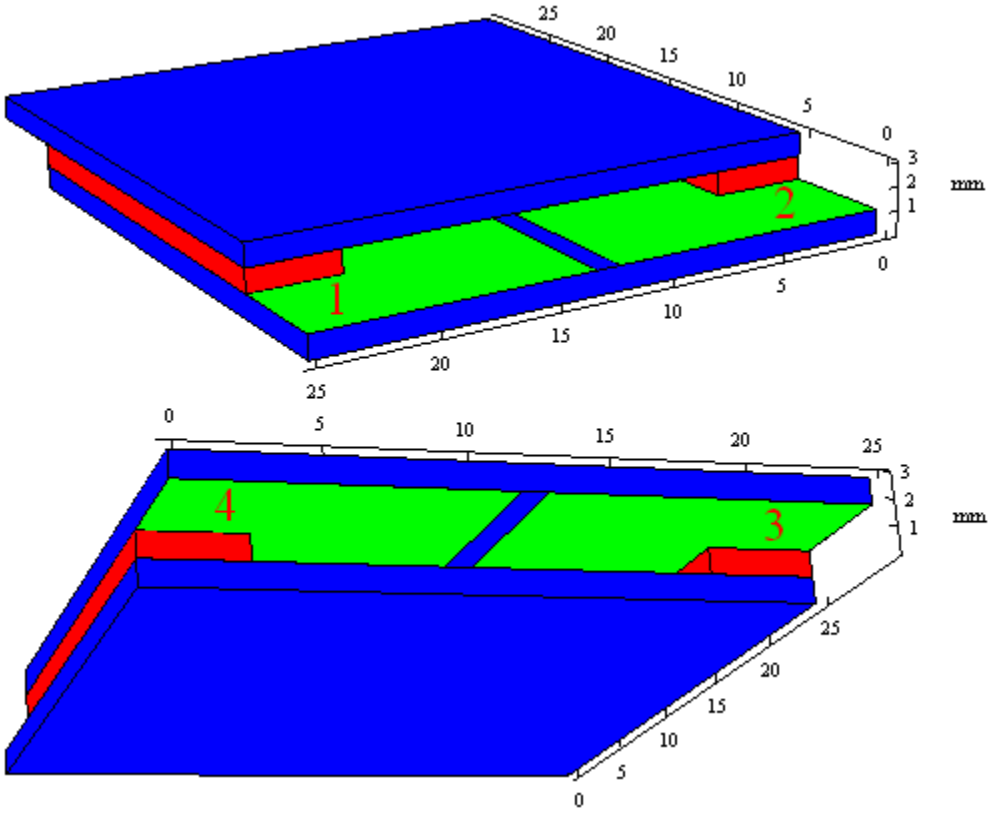

Figure 3.4: Front and back views of a completely assembled cell (from above and below, respectively). Colours explained in text.

spin coated, we use tape to prevent a small strip at the edge of the slide from being coated in lipid. This is so that the spacers will contact the glass directly, and not the lipid layer. We attach the top plate to the spacers using NOA 61, now making sure to cover the lipid area while curing, since our UV source would not only heat the lipid up (with unknown consequences) but also bleach the fluorescent dye. Once the top plate is attached, the electrical leads are attached using conductive tape, and tested with a multimeter to ensure that the leads are well connected, and the electrodes are still isolated from one another.

Since vesicle formation begins as soon as the cell is filled with water, we don't have time to seal the remaining two edges of the cell using UV glue. Instead, we seal these edges using vacuum grease, since it is highly viscous and prevents evaporation almost entirely, but can be quickly applied. The cell is filled, sealed, and we are ready to image.

For electroformation, we short electrode 1 with 2, and 3 with 4. This creates a field similar to what we would expect if the plates had not been etched. The field geometry will obviously differ near the centre of the cell, but this actually works to our advantage. Since vesicle formation is lessened in this area, we have created a "void" into which we can attempt to move vesicles with DC fields.

When the vesicles are fully formed, we reconnect our voltage output so that electrode 1 is shorted with 3, and 2 is shorted with 4. When a voltage is applied in this case, we assume that for some region near the centre of the cell, the field is uniform parallel to the plane of the plate, and perpendicular to the etched line. The exact form of the field can be found by solving Poisson's equation with the boundary conditions given by our electrode geometry. It has previously been shown that

electrodes arranged in this geometry produce large areas of uniform field suitable for data observation [12]. Even though we have created a region with the field conditions we're looking for, we note that since the fluid in the cell is in fact a continuum, field non-uniformities elsewhere in the cell may cause unexpected behavior.

A photo of a fully constructed cell is shown in figure 3.5. Note the blue marks on the top slide, indicating the region within which we assume the field is uniform. This is necessary since it is difficult to distinguish the ITO coated regions from the plain glass once the slide is filled.

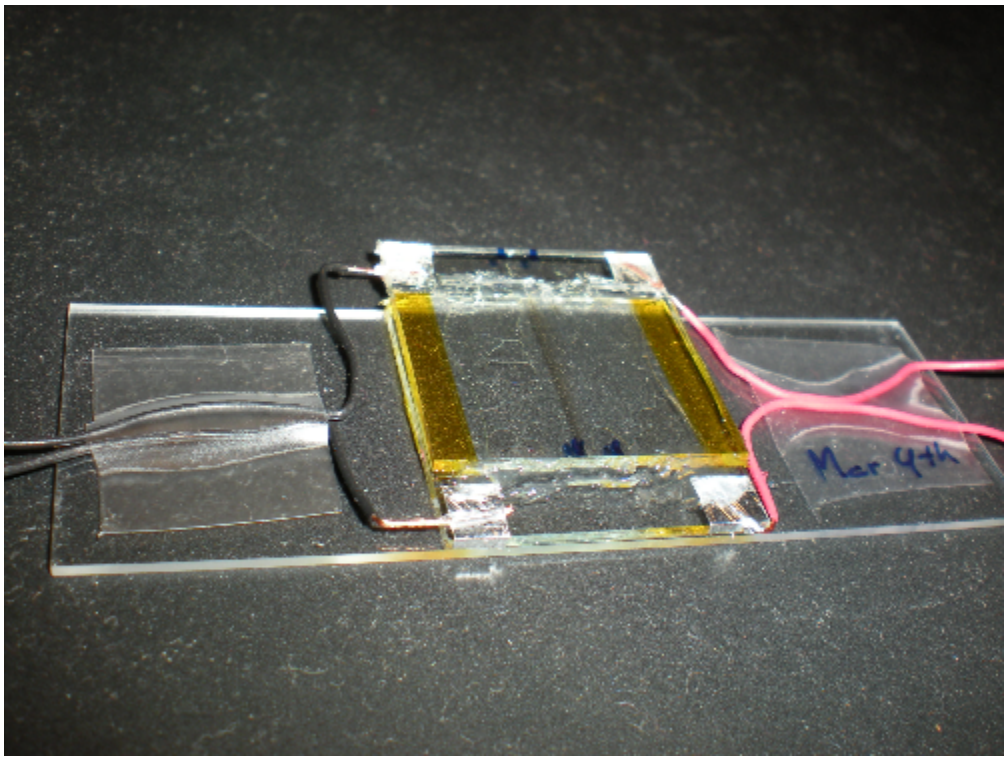

Figure 3.5: A photo of a cell, ready to electroform and image.

For our studies of colloids (section 4.3) our cell construction differs only slightly. The lipid layer is absent, so we need not worry about the time it takes to seal the cell and can therefore take the time to ensure the cell is well sealed. After filling the cell with colloid solution (specifics in section 4.3) we seal the remaining two ends of the cell using Norland UV Sealant 91 (UVS 91). This is a UV curable paste with a viscosity $\sim 50\,kcps$. To allow the sealant to fill any small gaps near the openings in the cell, we first place the entire cell on a hot plate at $50\,^{\circ}C$ for about a minute. Longer than this would cause undesirable evaporation of the colloid solution. When the glue comes into contact with the cell at this temperature, its viscosity decreases enough that it flows freely into the gaps in the cell, but not so much that it cannot span the $1\,mm$ cell spacing. While the glue is being cured under the mercury lamp, the colloid containing region is covered to reduce dye bleaching.

Chapter 4

Results

4.1 Vesicle Formation

Our vesicle formation procedure, as discussed in chapter 2 was quite successful in creating large, numerous EggPC vesicles. Figures 4.2 and 4.1 show confocal microscopy images of a cell following electroformation. Note that the vesicles are quite spherical in shape, and that the lipid membranes are highly contrasted against the solution. High quality vesicle formation was observed over the entirety of the lipid layer, and many vesicles also detached from the layer and diffused freely in the solution.

Two points of particular interest are labelled. Point A is a spot where the fluorescence seems quite high, but a vesicle membrane cannot be resolved. This may be due to the concentration of dye being too high, and crystallizing out of solution in certain places. Point B is a vesicle which is near the upper end of the size distribution. This vesicle has a measured diameter of $20.5\,\mu m$ (measured in ImageJ).

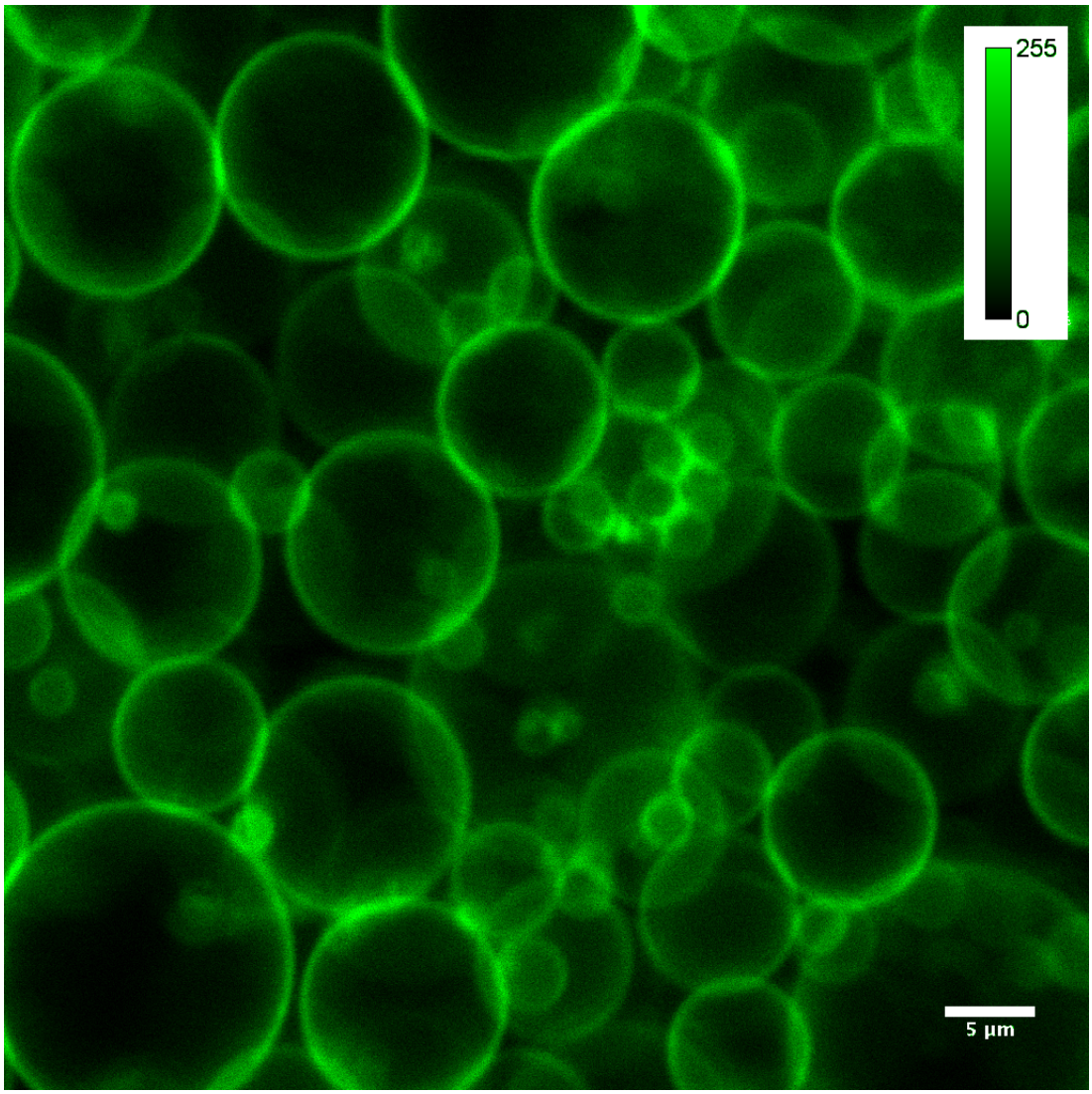

Figure 4.1: A fluorescent confocal microscopy image of EggPC vesicles at 40x magnification. Fluorescent dye is dissolved in the lipid which comprises the vesicle membranes.

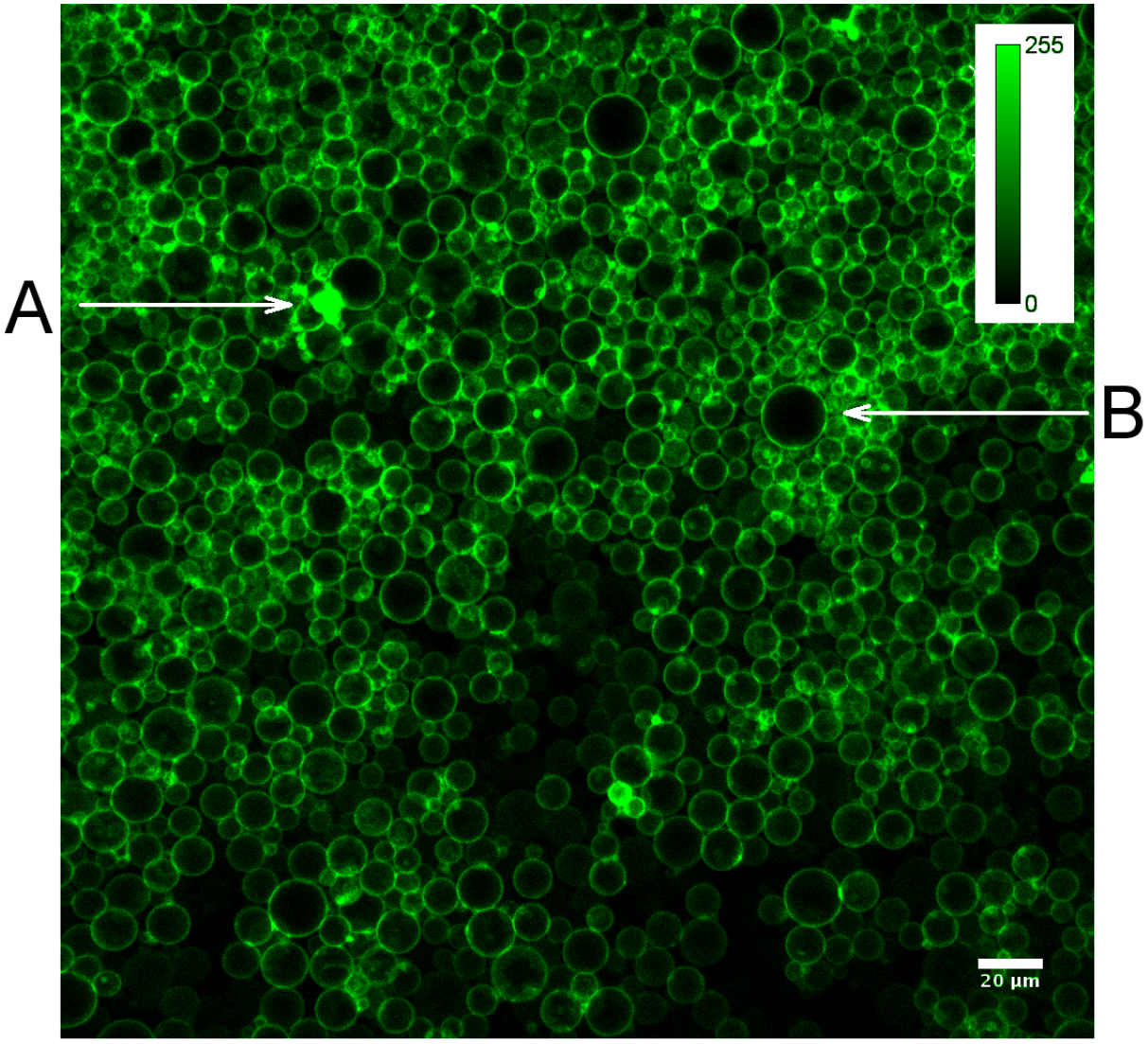

Figure 4.2: A fluorescent confocal microscopy image of EggPC vesicles at 10x magnification. Fluorescent dye is dissolved in the lipid which comprises the vesicle membranes.

The addition of the charged lipid, phosphatidylserine to our spin coating solution made a significant difference in the quality of the vesicles formed. It was obvious during electroformation that the presence of charged lipid was changing the effect of the AC field on the vesicles. While we have noticed that EggPC vesicles are slightly agitated by the electroformation field, the EggPC/PS vesicles showed a much stronger response. Once the vesicles reached a sufficient size that the membranous motions were easily visualized, we saw that the membranes were strongly oscillating at the AC frequency. There is no doubt that these strong fluctuations affected the final outcome of the vesicle formation. A more in-depth study of AC field effects on charged lipids will be required to re-optimize the electroformation process for this new lipid mixture. An image of the post-electroformation EggPC/PS vesicles is shown in figure 4.3.

It is clear that the quality of vesicle formation is significantly lower with the addition of phosphatidylserine, but that does not necessarily mean that that the vesicles are of no use to us. With a bit of searching in the cell, it was not difficult to find spherical vesicles which were freely diffusing. Red arrows in figure 4.3 indicate vesicles which are roughly spherical, and may be candidates for electrokinetic studies. With at least a few representative vesicles, we could a quantitative measure of the difference in response of pure EggPC vesicles and the EggPC/PS vesicles to DC fields.

We consider the possibility that the nature of the charged lipid is not the only source for the decrease in vesicle quality. The majority of the original vesicle formation work was done months before the purchase of the phosphatidylserine, so the EggPC used for the mixed lipid vesicles had been in storage for quite some

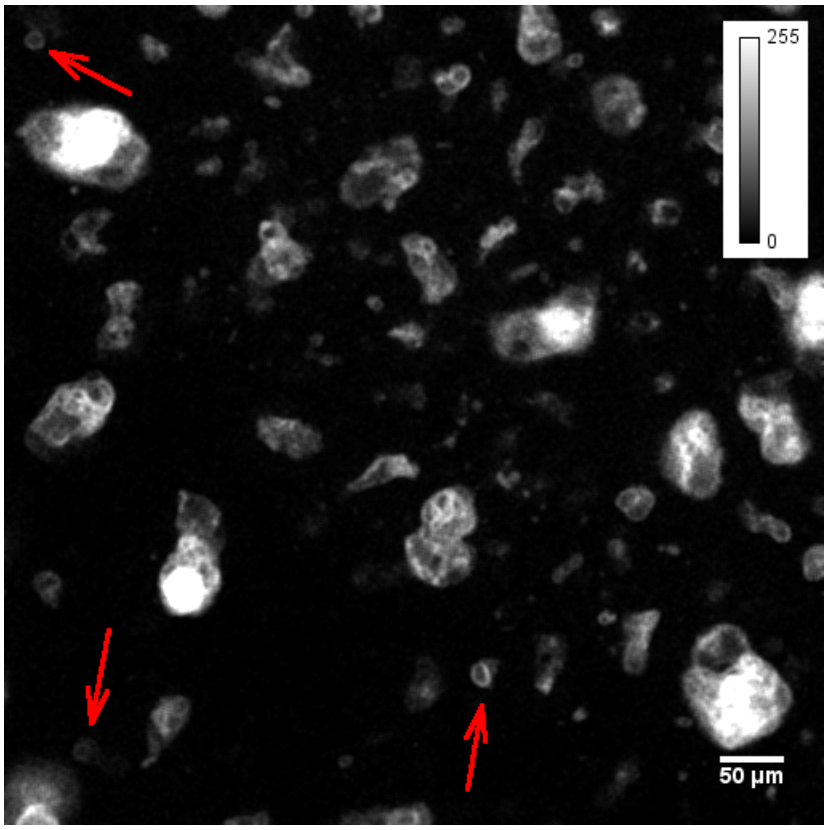

Figure 4.3: Vesicles composed of an 85/15 mixture of EggPC and phosphatidylserine, shown at 20x magnification. This image was taken after the electroformation field was turned off. Contrast is due to a fluorescent dye being excited under a mercury lamp.

time. Even though it was refrigerated, it may be that the EggPC degraded to some degree, affecting the quality of the vesicles.

4.2 Electrokinetics of Vesicles

After a qualitative test of our field setup (see discussion in section 4.3, specifically, figure 4.7) in which we saw that the field did in fact affect a colloid, we moved on to studying vesicles in the same setup.

We started with pure EggPC vesicles, but the response to the field was not as expected. We moved on to vesicles with PS added in the hope that a net charge on the vesicle would increase electrokinetic mobility. The response to DC fields was very similar for both types of vesicles (charged and uncharged).

Our vesicles responded to the applied fields. However, their response was not conducive to ABEL trapping. When the field was switched on, the vesicle would drift in the direction of the field until a certain time, when it would decelerate and stop. When the field was turned off, the vesicle would (in a similar amount of time) relax back to its original position. Figure 4.4 shows this behaviour for a

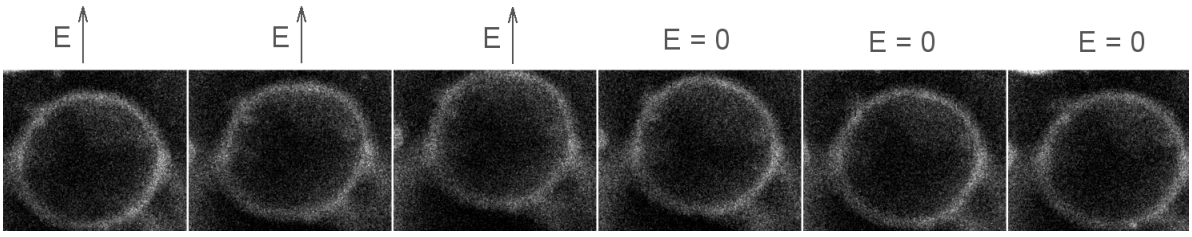

Figure 4.4: Time series images of a PC/PS vesicle under applied DC field of $1.0\,V\,mm^{-1}$.

field of $1.0\,V\,mm^{-1}$. This figure shows frames from a time series in which the field is applied and a single vesicle is imaged. The first frame coincides with the field being switched on, and the point at which the field is switched off is indicated.

This vesicle motion is quantified in figures 4.5 and 4.6. The first curve corresponds to the velocity in the time immediately after the field is switched on. It is fit to a decaying exponential function

$$v(t) = \alpha + \beta e^{-t} \tag{4.1}$$

where the fit parameters are $\alpha = -1.02\,\mu m\,s^{-1}$ and $\beta = 9.97\,\mu m\,s^{-1}$, with a regression coefficient $R^2 = .992$. This exponential form could be an indication that the fluidic drag force is dominating the vesicle motion. We allow the vesicle to reach a steady state, where its velocity is zero before turning the field off. The second curve (figure 4.6) shows the vesicle velocity after the same DC field is switched off. Note that in this case, the vesicle accelerates for some time (until $\sim 0.5\,s$) and then decelerates in a manner similar to when the field was switched on. The fit on this curve is performed excluding the first point, and has fit parameters: $\alpha = -0.46\,\mu m\,s^{-1}$, $\beta = 5.90\,\mu m\,s^{-1}$ and regression coefficient $R^2 = .988$.

We see that the offset of the vesicle while the field is applied is proportional to the field strength, but the relaxation to the original position is independent of field strength and occurs over all field strengths we examined (0 up to $2.5\,V\,mm^{-1}$.)

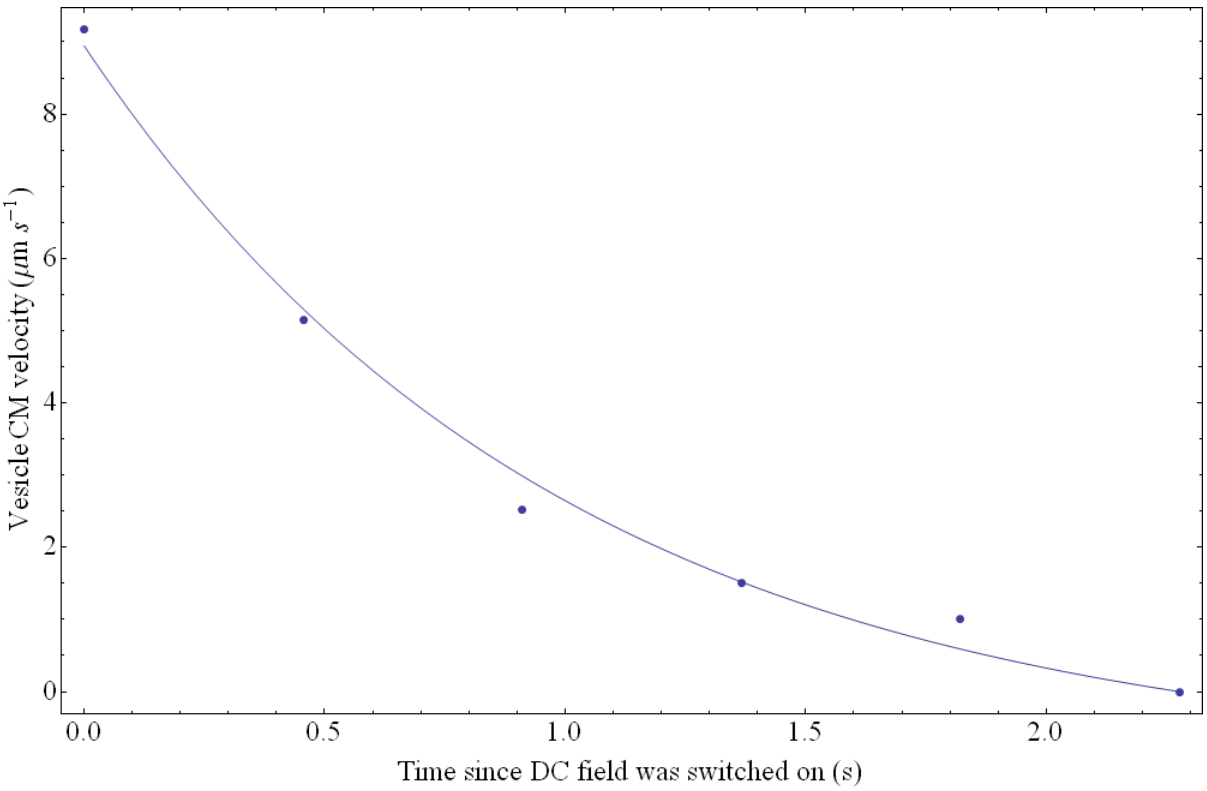

Figure 4.5: Vesicle velocity immediately after a $1.0\,V\ mm^{-1}$ is switched *on*. Fit curve is described in text.

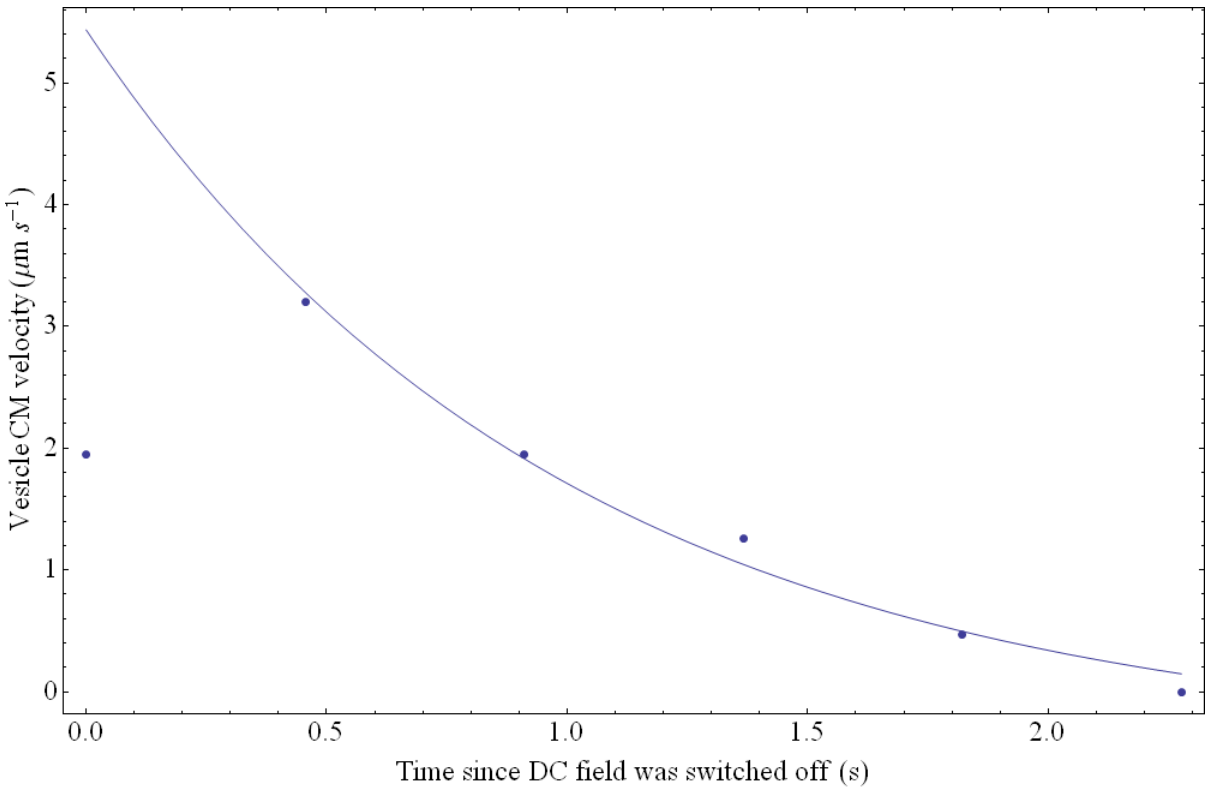

Figure 4.6: Vesicle velocity immediately after a $1.0\,V\ mm^{-1}$ is switched *off*. Fit curve is described in text.

4.3 Electrokinetics of Colloids

After our proof of concept (see section 3.3) was successful we decided to not begin with electrokinetic studies of vesicles, but rather start with a simpler system and check to see that our electric field was behaving as expected. For this simplified particle, we chose colloidal polystyrene spheres of $1\,\mu m$ diameter. Our first test cell used a $30\,\mu m$ cell spacing, and we applied fields ranging from $0.1\,V\,mm^{-1}$ to $0.6\,V\,mm^{-1}$. The cell construction was less than ideal, and evaporation-induced flow was apparent over the entire cell, but we were looking for a qualitative result: do the colloids respond to the field? Figure 4.7 shows the result of this test for the $0.6\,V\,mm^{-1}$ field. These images are produced from time series, averaged over about $5\,s$, resulting in chain-like features which actually represent velocity vectors. The motion due to the fluid flow is much greater than that induced by the DC field but there is an obvious change in the direction of particle motion in the direction of the applied field. This indicates that we are applying a field, and it *is* affecting the colloids.

For such an imperfect system, we can make few assumptions about why, but it is important to note that when the DC voltage was switched off, the flow relaxed back to its original direction. This became a recurring behavior in all consequent cells, both with colloids and vesicles.

After some time studying vesicles (discussed in section 4.2), we returned to colloids in an attempt to gather more quantitative data. We moved to a $1\,mm$ cell spacing to more closely mimic our vesicle cell, but altered our spacer geometry. Our reasons for this alteration are discussed in chapter 5; here we will just say that

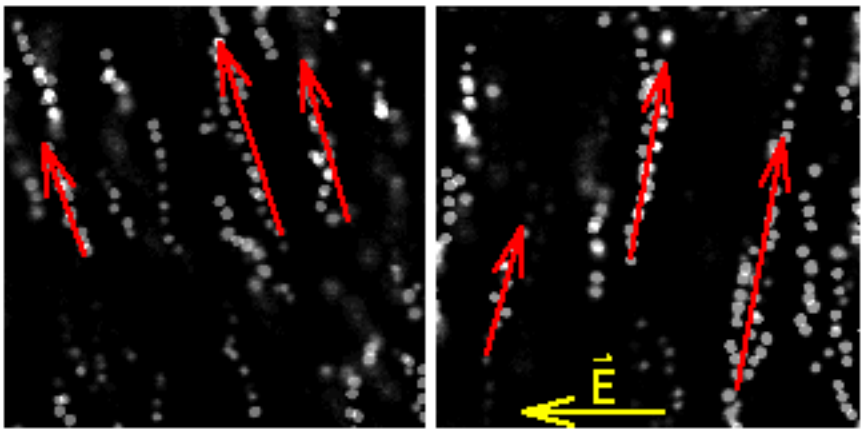

Figure 4.7: The effect of a $0.6\,V\,mm^{-1}$ DC field on $1\,\mu m$ polystyrene spheres. Images further explained in text.

we move the spacers inward, until their edges coincide with the edges of the ITO layer. Figure 4.8 shows this new cell design.

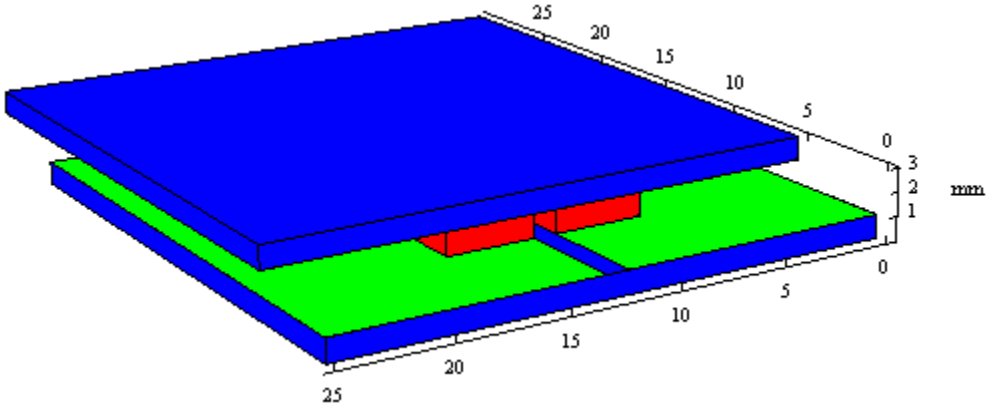

Figure 4.8: A revised colloid cell design (compare to figure 3.4). In this cell, the electrodes are completely isolated from the aqueous solution.

The principle difference in outcome of the revised cell was that there was no net

flow without a field being applied. Also, since the electrodes have been removed from the solution, we can apply higher voltages without the possibility of electrochemical reactions occurring on the electrodes. We observed similar results to the previous cell, in that the applied field seemed to induce some preferred direction of motion in addition to the Brownian motion of the particles. To some extent, we still see a "relaxation" of the particles towards their original positions when the field is switched off. This data is analysed in the same manner as the previous colloid cell and shown in figure 4.9. Averaged over $10\,s$, we see that not only is there a preferred direction of motion with the field applied, but the magnitude of the displacement is greatly increased.

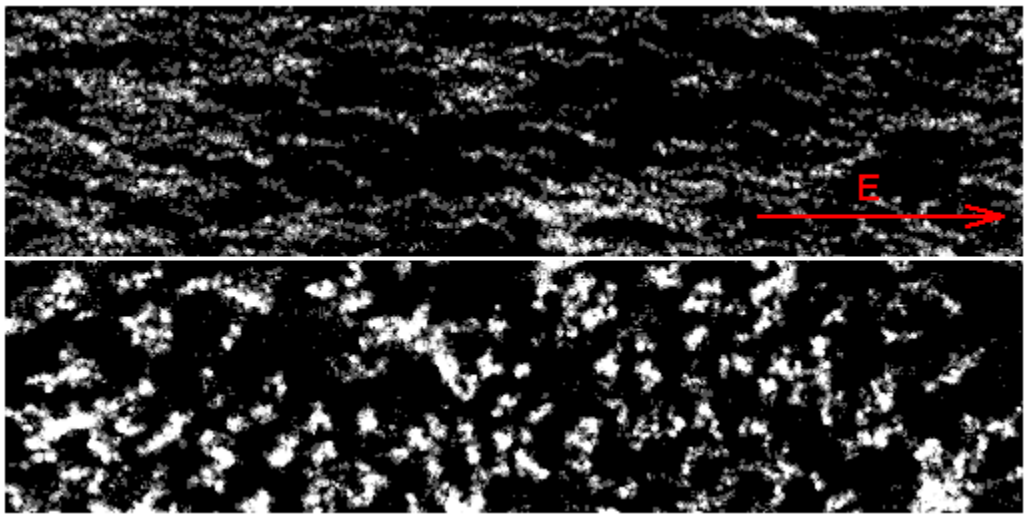

Figure 4.9: Time averaged images of polystyrene using our revised cell design. Averaged over $10\,s$. The bottom image corresponds to no field, and the top image is in the presence of a DC field of $2.5\,V\,mm^{-1}$

Figure 4.10 is an analysis of the electrokinetic mobility of the colloids shown

in figure 4.9. The velocities plotted are averaged over all particles in the field of view. Both x and y velocities are plotted. The two obvious discontinuities in the velocities correspond to the DC field being switched on and off, respectively. When the field is switched on, the x velocity jumps to approximately $4.0\,\mu m\,s^{-1}$, and then decays asymptotically to some steady state velocity. Once this steady state is reached, the field is switched off, causing the x component of the velocity to switch direction. This negative velocity moves the colloids back towards their original positions (before the field was turned on). This velocity decays to zero, and the motion of the particles assumes its original form. Since the area under the curve for the positive velocity is greater than the area under the negative region of the curve, the net motion of the particles due to the field is positive.

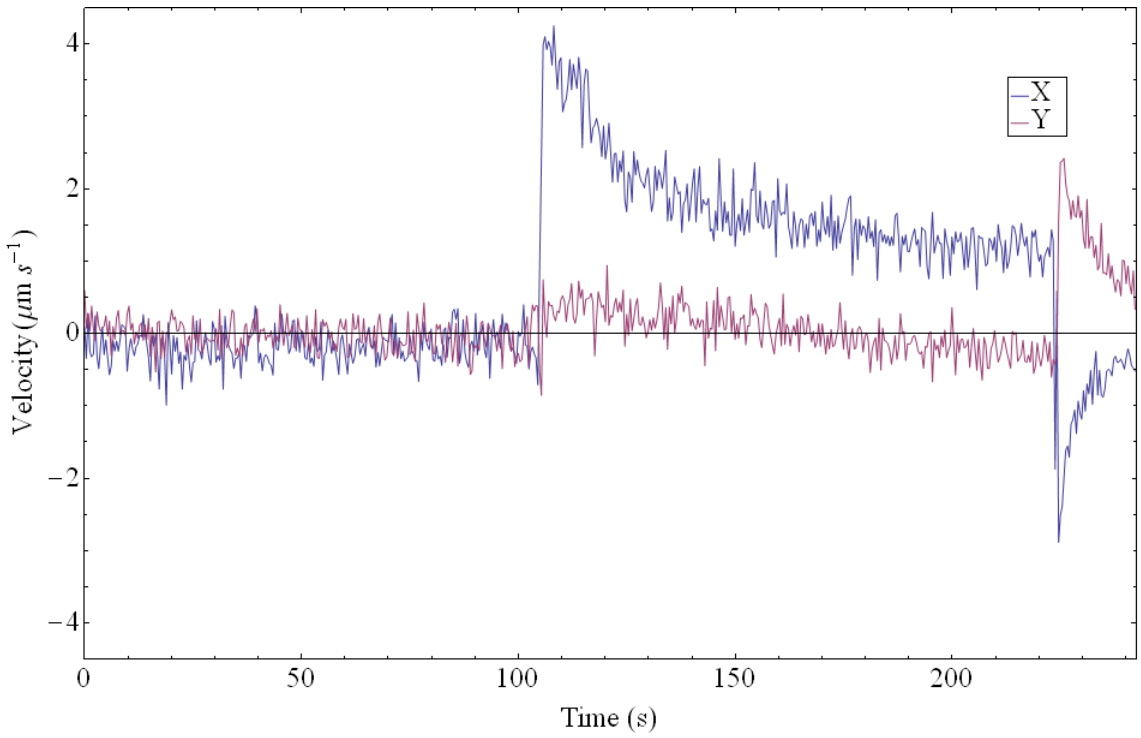

Figure 4.10: Electrokinetic mobility of $1\,\mu m$ polystyrene spheres. Discontinuities correspond to a $2.5\,V\,mm^{-1}$ DC field being turned on and off, respectively. The field is applied in the x direction.

Chapter 5

Summary and Conclusions

Our first goal was to optimize a process for the production of phospholipid vesicles. We then intended to design an apparatus to study the electrokinetic mobility of these vesicles by applying various DC electric fields and measuring vesicle velocities. With an understanding of the electrokinetic mobility of the vesicles, we hoped to offset their Brownian motion by tracking their motion and applying DC electric fields in a feedback loop.

While we did not achieve the ultimate goal of ABEL trapping vesicles, we certainly have a better feeling for the types of issues that arise in such a system. The construction of the apparatus and integration with the LabVIEW code was accomplished, and while the frequency of trapping is only $1\,Hz$, we should be able to at least confine particles to some area, proportional to their rate of diffusion.

Table 5.1 is a chronological summary of different cells discussed in this thesis, including their contents, cell spacing, electrode geometry, and any results or additional comments.

Table 5.1: Summary of Samples Studied

Contents	Cell Spacing	Electrode Geometry	Results/Comments
EggPC	$1\,mm$	Neither plate etched	Original electroformation setup
Colloid	$30\,\mu m$	Bottom plate etched, glass plate on top	Flow due to evaporation issues. Fig 4.7.
EggPC	??	Etched bottom plate, un-etched top plate	First observation of "relaxation" after DC field switched off.
PC/PS	$30\,\mu m$	Both plates etched	Cell volume much too small to allow vesicles to swell to full size.
PC/PS	$1\,mm$	Both plates etched	Electroformation not optimized, poor formation results. Air bubbles in cell.
Colloid	$1\,mm$	Both plates etched	Revised cell design (fig 4.8). No flow, relaxation minimal

The vesicles formed from our EggPC/PS mixture were not of the same quality as those formed from pure EggPC in terms of number, size, or shape. We will need to conduct a systematic study of the response of PC/PS vesicles to AC electric fields and re-optimize our electroformation process. Only after this is accomplished can we make any conclusions about which lipid is more feasible for electrokinetic trapping.

The "relaxation" behaviour we have observed occurred in two different types of lipid vesicles as well as with our initial colloid studies, but its extend was lessened in the last colloid cell (revised cell design). This leads us to the conclusion that the revised cell design was in fact and improvement, and gives us a direction in which to plan further cell design changes. Since our cell was originally designed for electroformation, and then modified to also apply DC fields in a perpendicular direction, it may be that we need to re-think our cell design to allow application of fields of larger magnitudes. This would involve moving our electrodes closer together, which is not easily accomplished in our electroformation cell. One option we have considered is forming vesicles in a separate cell, and pipetting them into the trapping cell. This has the advantage of allowing us to form vesicles at a high concentration and then dilute them to a concentration more suitable for isolating single vesicles. Another reason for this change is that it simplifies the cell construction: the lipid won't be present in the cell when the spacers and top plate are glued, so it doesn't risk being exposed to UV light. Since the vesicles would be added in the last stage of cell construction, we no longer need to rush to construct the cell, and could consider more options in terms of adhesives (such as a two-component epoxy).

While we don't have a definite reason for the unusual response to the DC fields, we consider a few possibilities. First, our assumption that the field is uniform in some region near the centre of the cell is likely a good one, but we hadn't considered the possibility that field gradients elsewhere in the cell could induce fluid flows that would affect the entire cell, including the region we're imaging. This makes sense since water is dipolar and would experience dielectrophoretic forces in any region of the cell where the field is non-uniform. We could remedy this in a few ways, the most obvious of which is to devise a field which is perfectly uniform over the entire region containing water. This may be difficult in practise, but it will be a consideration in any future cell designs.

While the principle reason for our revised colloid cell (figure 4.8) was to ensure field uniformity across the entire cell, the design has a few features which will be useful in future cells. It seems that the smaller cell was easier to seal, thereby avoiding evaporation-induced flow. The smaller area of the cell also means that is it less likely to have air bubbles form while filling and sealing it. The dielectric mismatch between air and water would cause field non-uniformities near any bubbles in the cell, so they must be avoided if we are to assume uniform fields throughout the cell. The colloid cell produced electrokinetic drift much closer to that which we require for trapping, in that the net displacement after the field was removed was greater than zero, and proportional to the field applied. With reference to figure 4.10, the region of highest response is that immediately after the field is switched on. This is exactly what we would hope for, since in an ABEL trapping situation the field will be changing much to quickly for long timescale relaxation effects to matter.

Our main intention for future work is to scale the size of the trap downwards. By doing so we decrease the amount of fluid we need to keep track of, and reduce the possibility of distance effects changing flows in our trapping region. Primarily, however, a smaller electrode spacing would also allow us to apply larger fields using smaller voltages. When we started our electrokinetic studies, it made sense to start with small fields and work our way up, and it may be that we just never made it to the point where "snappy" response to the field is observed. The trap upon which this work is based cites fields an order of magnitude larger than those we have been using ($\sim 25\,V\,mm^{-1}$ as opposed to our $2.5\,V\,mm^{-1}$) [5]. By scaling down, we can observe vesicle mobility under larger fields without electrochemical reactions on the electrodes ever becoming an issue. While we have not constructed a functional ABEL trap, we believe that it is a feasible method for studying bilayer membranes, and intend on continuing our electrokinetic studies to this end.

Bibliography

[1] M. I. Angelova and D. S. Dimitrov. Liposome electroformation. *Faraday Discussions of the Chemical Society*, 81:303–311, 1986.

[2] M. I. Angelova, S. Solau, P. Mlard, F. Faucon, and P. Bothorel. Preparation of giant vesicles by external ac electric fields. kinetics and applications. *Progress in Colloid and Polymer Science*, 89:127–131, 1992.

[3] A. Ashkin, J. Dziedzic, J. Bjorkholm, and S. Chu. Observation of a single-beam gradient force optical trap for dielectric particles. *Optics Letters*, 11:288–290, 1986.

[4] D. Cherney, T. Bridges, and J. Harris. Optical trapping of unilamellar phospholipid vesicles: Investigation of the effect of optical forces on the lipid membrane shape by confocal-raman microscopy. *Analytical Chemistry*, 76:4920–4928, 2004.

[5] A. E. Cohen and W. E. Moerner. An all-glass microfluidic cell for the abel trap: fabrication and modeling. *Proc. SPIE*, 5903:191–198, 2005.

[6] A. E. Cohen and W. E. Moerner. Suppressing brownian motion of individual biomolecules in solution. *Proceedings of the National Academy of Sciences (PNAS)*, 103(12):4362–4365, 2006.

[7] D. S. Dimitrov and M. I. Angelova. Lipid swelling and liposome formation on solid surfaces in external electric fields. *Progress in Colloid and Polymer Science*, 73:48–56, 1987.

[8] R. Dimova, K. A. Riske, S. Aranda, N. Bezlyepkina, R. L. Knorr, and R. Lipowsky. Giant vesicles in electric fields. *Soft Matter*, 3, 2007.

[9] A. Einstein. Zur theorie der brownschen bewegung. *Annalen der Physik*, 17:549–560, 1906.

[10] D. J. Estes and M. Mayer. Electroformation of giant liposomes from spin-coated films of lipids. *Colloids and Surfaces B: Biointerfaces*, 42(2):115–123, 2005.

[11] R. Glaser. *Biophysics*. Springer, 2005.

[12] N. Li. Colloidal ordering under external electric fields. Master's thesis, Memorial University, St. John's, NL, 2008.

[13] Lodish, Berk, Kaiser, Krieger, Scott, Bretscher, Ploegh, and Matsudaira. *Molecular Cell Biology*. Freeman, sixth edition edition, 2008.

[14] K. A. Riske and R. Dimova. Electric pulses induce cylindrical deformations on giant vesicles in salt solutions. *Biophysical Journal*, 91:1778–1786, 2006.

[15] C. J. R. Sheppard and D. M. Shotton. *Confocal Laser Scanning Microscopy*. BIOS Scientific Publishers Ltd., 1997.

[16] E. Soussan, S. Cassel, M. Blanzat, and I. Rico-Lattes. Drug delivery by soft matter: Matrix and vesicular carriers. *Angewandte Chemie International Edition*, 48:274–288, 2009.

[17] Wikipedia. Lipid bilayer — wikipedia, the free encyclopedia, 2009. [Online; accessed 15-March-2009].

[18] Wikipedia. Phospholipid — wikipedia, the free encyclopedia, 2009. [Online; accessed 15-March-2009].

Appendix A: LabVIEW Code

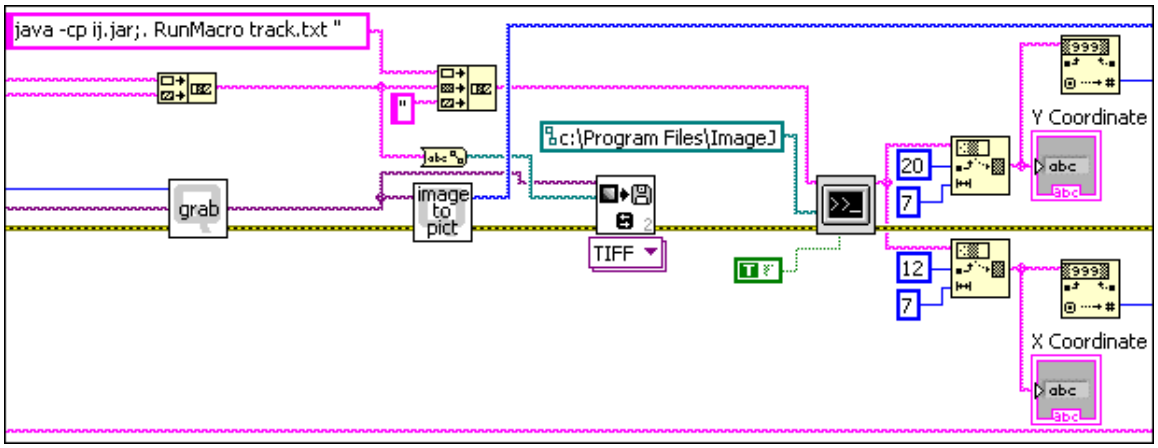

Figure 5.1: LabVIEW block diagram for ABEL trap, part 1: "Grab" image from the camera, run ImageJ (see 3.2.2 for details), and extract feature coordinates from standard output.

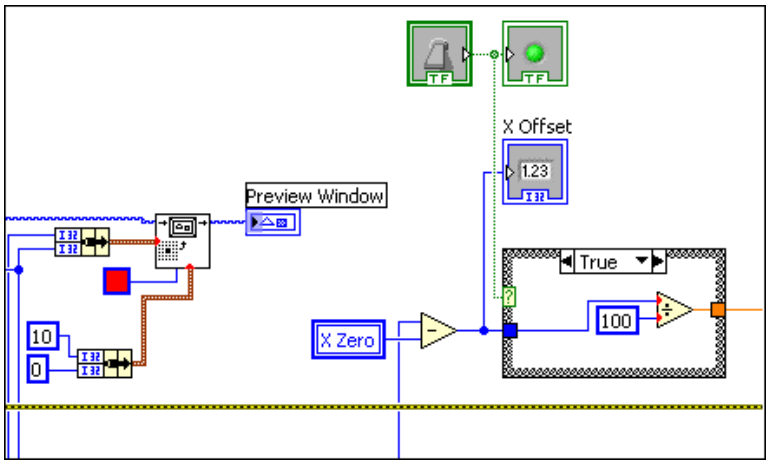

Figure 5.2: LabVIEW block diagram for ABEL trap, part 2: Overlays a red dot on the image at the location of the feature centre. Voltage is computed from the particle offset.

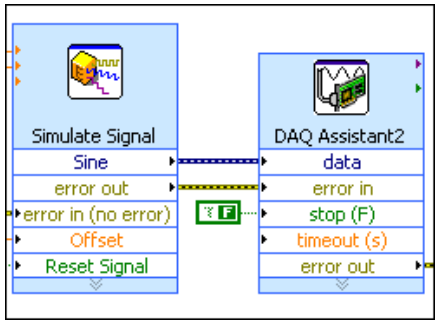

Figure 5.3: LabVIEW block diagram for ABEL trap, part 3: Simple "black box" functions take input parameters such as frequency, amplitude and offset and generate a voltage waveform. This is then sent to the voltage output card (see 3.1.2)

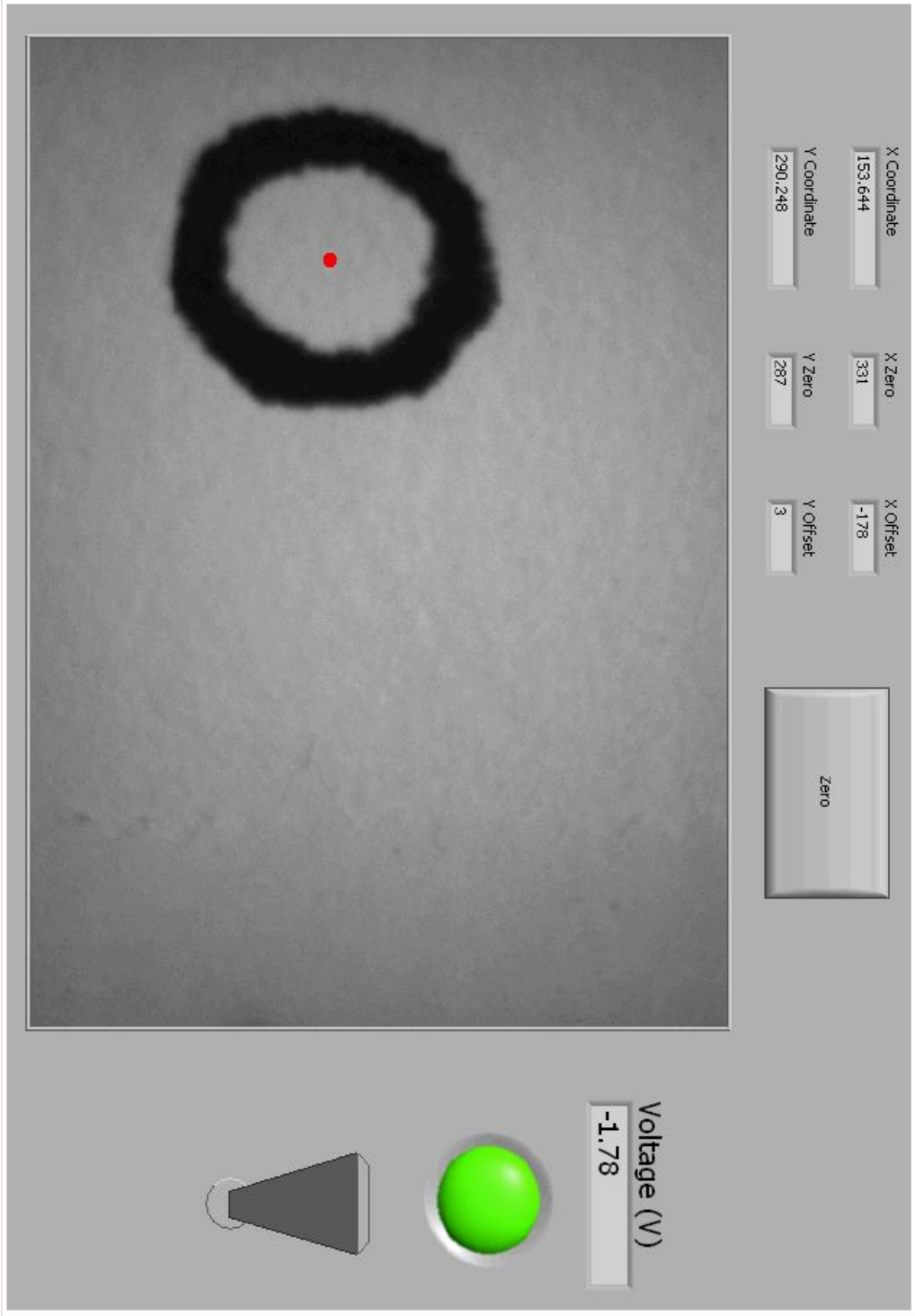

Figure 5.4: LabVIEW front end for ABEL trap. Image is rotated to fit. The green light indicates that the voltage output is active.

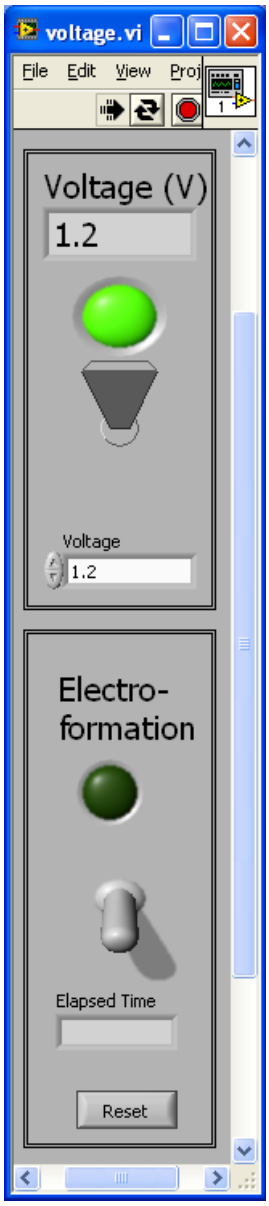

Figure 5.5: LabVIEW front end for streamlined voltage output code. This version of the LabVIEW code was used for the electrokinetics studies. Note that the DC voltages can be replaced with a sine wave for electroforming vesicles with the flip of a switch.